G-Quadruplex Folds of the Human Telomere Sequence Alter the Site Reactivity and Reaction Pathway of Guanine Oxidation Compared to Duplex DNA

*Aaron M. Fleming and Cynthia J. Burrows**

Department of Chemistry, University of Utah, 315 South 1400 East, Salt Lake City, Utah,

United States 84112-0850

*To whom correspondence should be addressed. Phone: (801) 585-7290. Fax: (801) 585-0024.

E-mail: burrows@chem.utah.edu.

Supporting Information

Page

Complete Methods.....S4

Figure S1. Representative CD spectra for the contexts studied……..S7

Figure S2. T_m values for each ODN context studied……..S8

Figure S3. Native gel electrophoresis for the contexts studied……..S9

Figure S4. Representative storage-phosphor autoradiogram for the G-quadruplex oxidation sites with riboflavin…….....S10

Figure S5. Representative storage-phosphor autoradiogram for the duplex oxidation sites with riboflavin…….S11

Figure S6. Representative storage-phosphor autoradiogram for the duplex oxidation sites with Rose Bengal……S12

Figure S7. Comparison of oxidation sites for reactions conducted with and without NAC……..…S13

Figure S8. Oxidation sites and products observed in the hybrid and basket folds utilizing the one-electron oxidant Na_2IrCl_6……...…S14

Figure S9. Method for determining the product distributions…….S15

Figure S10. Standard curve for Ellman's free thiol concentration test…….……..S16

Figure S11. Time-dependent concentrations of NAC during the oxidation reactions……...….S17

Figure S12. Hunt for a G*-T* crosslink…….…....S18

Figure S13. Oxidation sites observed for the propeller-like folded G-quadruplex……..…..S19

Figure S14. CD Spectra for G-quadruplexes in the presence of riboflavin……..…..S20

Figure S15. CD and T_m characterization of the double G-quadruplex……...…S21

Figure S16. Gel-electrophoresis analysis of double-G-quadruplex oxidations with Rose Bngel ($^1O_2$)…….…….S22

Figure S17. Characterization of G-quadruplexes in mixed salts……....S23

Figure S18. G-Quadruplex oxidation sites in mixed salt buffers…….....S24

Figure S19. Reevaluation of the Sp and Gh extinction coefficients……...S25

Figure S20. Comparison of reaction sites for the hybrid and basket folds…….S26

Figure S21. Comparison of reaction sites for the natural human telomere sequence and the locked telomere sequence…….S27

Figure S22. Relative product distributions for the contexts studied……..…..S28

References…….…...S29

Complete Methods

The ODNs were purified by semi-preparative HPLC on a Dionex DNAPac ion-exchange column in which mobile phase A = 10% CH_3CN/90% ddH_2O, and B = 25 mM LiOAc (pH 7) 1 M LiCl and 10% CH_3CN/90% ddH_2O running at 3 mL/min while monitoring the absorbance at 260 nm. Next, the excess salts were removed by dialysis. The ODN concentrations were determined by UV-vis in ddH_2O at 75 ^oC utilizing the following extinction coefficients: ε (5'-TAGGG(TTAGGG)$_3$TT) = 0.2805 L*μmole^{-1}*cm^{-1}, and ε (5'- ATA TTA TTA GGG TTA TTA TTA) = 0.2349 L*μmole^{-1}*cm^{-1}. Annealing occurred by heating the ODN samples at a 10.0 μM concentration in reaction buffer to 90 ^oC followed by slowly cooling them to room temperature (~3 h); next the G-quadruplex samples were kept at 4 ^oC for 48 h prior to their study. The reaction buffer consisted of 20 mM MP_i (pH 7.4) 120 mM MCl (M = Na or K). 5'-^{32}P labeling was conducted as previously described.[1] T_m analysis was conducted by monitoring the absorbance at 260 nm for duplex samples, and 295 nm for G-quadruplex samples, at a 3.0 μM concentration while heating the samples from 15.0 to 85.0 ^oC at a ramp rate of 0.3 ^oC/min, and a measurement was taken every minute. Native gel electrophoresis was conducted on the 5'-^{32}P labeled ODNs in a 15% polyacrylamide gel doped with 120 mM MOAc (M = Na or K) in the gel and running buffer. The samples were electrophoresed at 20 W for 12 h while maintaining the temperature at 23 ^oC, and the bands were visualized by storage-phosphor autoradiography on a phosphorimager.

^{32}P Labeling Reaction. The ODN strands were 5' labeled with ^{32}P for visualization on a PAGE gel using storage phosphor autoradiography. Labeling of the ODN was conducted by mixing 100 pmoles of ODN in 37 μL of ddH_2O, 2 μL of T4-polynucleotide kinase (T4-PNK), 5 μL of 10X PNK buffer (does not contain monovalent cations), and 6 μL of [γ-^{32}P]-ATP (30 μCi).

The labeling proceeded for 1 h at 37 ^{o}C. Next, the entire sample was placed into a G-25 spin X column (GE Healthcare) and centrifuged following the manufacturer's protocol to remove excess [γ-^{32}P]-ATP. The resulting sample was diluted to 250 μL to obtain a suitable concentration of radioactivity. The extent of ^{32}P incorporation was quantified using a scintillation counter. In reactions where PAGE analysis was used, 20,000 cpm of labeled ODN was added to each reaction sample prior to annealing.

Complete Nuclease Digestion Protocol. The ODN samples were digested with a suite of nucleases to liberate the oxidized nucleotides as follows: (1) The antioxidant butylated hydroxytoluene (2.0 mM) along with the deaminase inhibitors pentostatin (100 μM) and tetrahydrouridine (100 μM) were added before commencement of the digestion. The ODN samples were lyophilized to dryness and then resuspended in DNase I reaction buffer (20.0 mM Tris (pH 8.4), 2.0 mM $MgCl_2$, 50.0 mM KCl) followed by addition of DNase I (2.0 U), and incubated at 37 ^{o}C for 3 h. (2) 10-μL of a NaOAc buffer solution (100.0 mM, pH 5.3) containing zinc acetate (10.0 mM) was added to the digestion solution, followed by nuclease P1 (2.0 U). The reaction was incubated at 45 ^{o}C for 9 h, followed by addition of more nuclease P1 (2.0 U) and incubation for another 9 h. (3) 11-μL of tris buffer (100.0 mM, pH 7.8) with $MgCl_2$ (10.0 mM) and snake venom phosphodiesterase (2.0 U) was added to the digestion mixture. The reaction was incubated at 45 ^{o}C for 9 h after which snake venom phosphodiesterase (2.0 U) and calf intestinal phosphatase (16.0 U) were added and allowed to react for 9 h to liberate the damaged and undamaged nucleosides from the reacted ODNs. The digestion proteins were removed before HPLC analysis by passing the sample through a 10,000 molecular weight cutoff filter (Millipore), and then analyzed by HPLC as follows below.

Complete HPLC Methods for Digested ODNs. Analysis of the digestion reactions was conducted by passing the sample down a C18 reversed-phase HPLC column (250 X 4.6 mm, 5 μm) running the following solvents: A = 10 mM NH_4OAc (pH 7.0) in ddH_2O, B = CH_3CN, running at 1 mL/min, while monitoring the absorbance at 240 nm. The run was initiated at 1% B then after 3 min B increased to 10% over 10 min following a linear gradient, after which 10% B was held isocratic for 4 min. Next, B was increased to 65% over 10 min along a linear gradient then held at 65% for 10 min followed by termination of the run. The void volume from this HPLC run was collected and lyophilized to dryness.

Analysis of the void volume from the previous run was achieved by passing the collected sample down a Hypercarb HPLC column (150 X 4.6 mm, 5 μm, Thermo Scientific) that was running the following solvent systems: A = 0.1% acetic acid in ddH_2O, and B = methanol, while running at a 1 mL/min flow rate, and monitoring absorbance at 240 nm. The run started at 0% B and after 10 min increased to 90% B following a linear gradient over 30 min.

CD Spectrum with 140 mM K^+

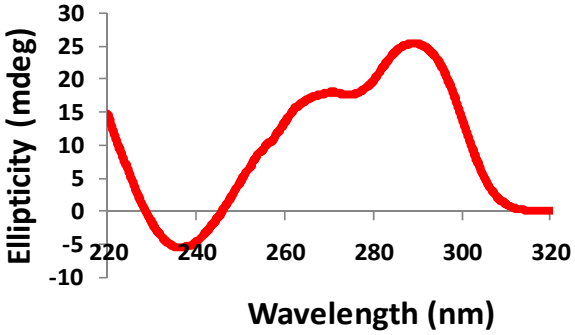

CD Spectrum with 140 mM Na^+

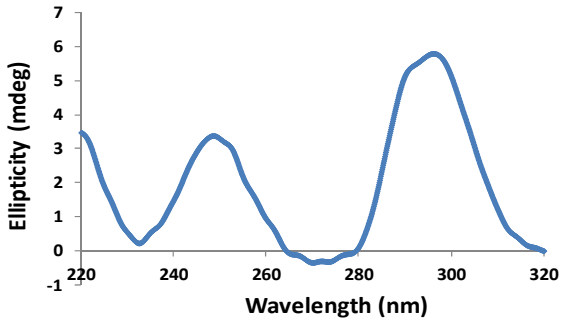

CD Spectrum with 140 mM K^+; 50% CH_3CN in H_2O

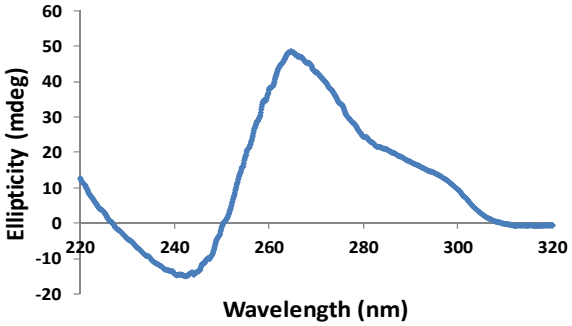

Figure S1. Representative CD spectra for the contexts studied. The sequence 5'-d(TAGGGT)$_4$T-3' was evaluated under the various conditions. The data were recorded on a 10 μM ODN solution in 20 mM MP_i (pH 7.4) with 120 mM MCl (M = Na or K) at 20 ^oC.

Typical G-Quadruplex Melting Profile

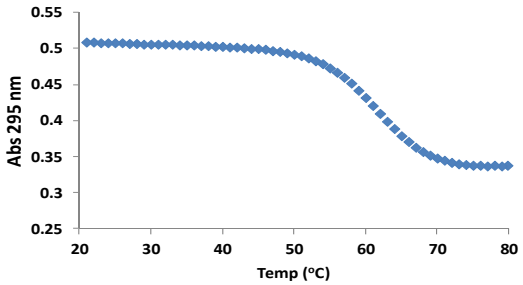

Structure	T_m (°C)*
Hybrid (KCl)	60.0 ± 1.0
Basket (NaCl)	52.3 ± 0.7
Propeller (KCl + 50% CH_3CN)	53.7 ± 0.9
Duplex (KCl)	51.9 ± 0.8

*The duplex T_m was determined by monitoring the absorbance at 260 nm vs. temperature, and the G-quadruplex T_m values were determined by monitoring the absorbance at 295 nm vs. temperature. The T_m values were determined from the inflection point in the melting process.

The data were recorded on a 3 μM ODN solution in 20 mM MP_i (pH 7.4) with 120 mM MCl (M = Na or K).

Figure S2. T_m values for each ODN context studied.

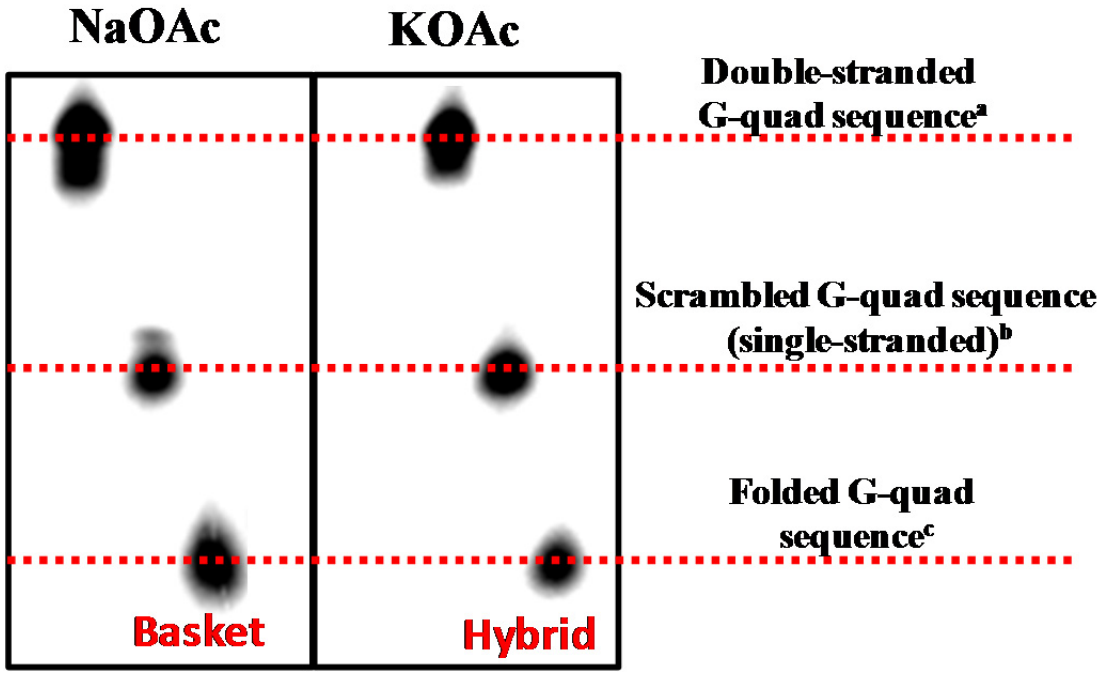

[a] The G-quad sequence 5'-TAGGG(TTAGGG)$_3$TT-3' was annealed to its complementary strand 3'-ATCCC(AATCCC)$_3$AA-5' forming a duplex. [b] The scrambled G-quad sequence 5'-TGAGTGTGAGTGTGAGTGTGAGTGT-3' was studied, which cannot fold to a quadruplex structure and gives a single-stranded control strand. [c] The G-quadruplex sequence 5'-TAGGG(TTAGGG)$_3$TT-3' was studied by ion-dependent native gel electrophoresis in which the gel in the left panel was doped with 120 mM NaOAc, and the gel in the right panel was doped with 120 mM KOAc, to give the basket and hybrid folds, respectively. The gels were conducted at 23 ^{o}C, and electrophoresed for 12 h at 20 W.

Figure S3. Native gel electrophoresis for the contexts studied.

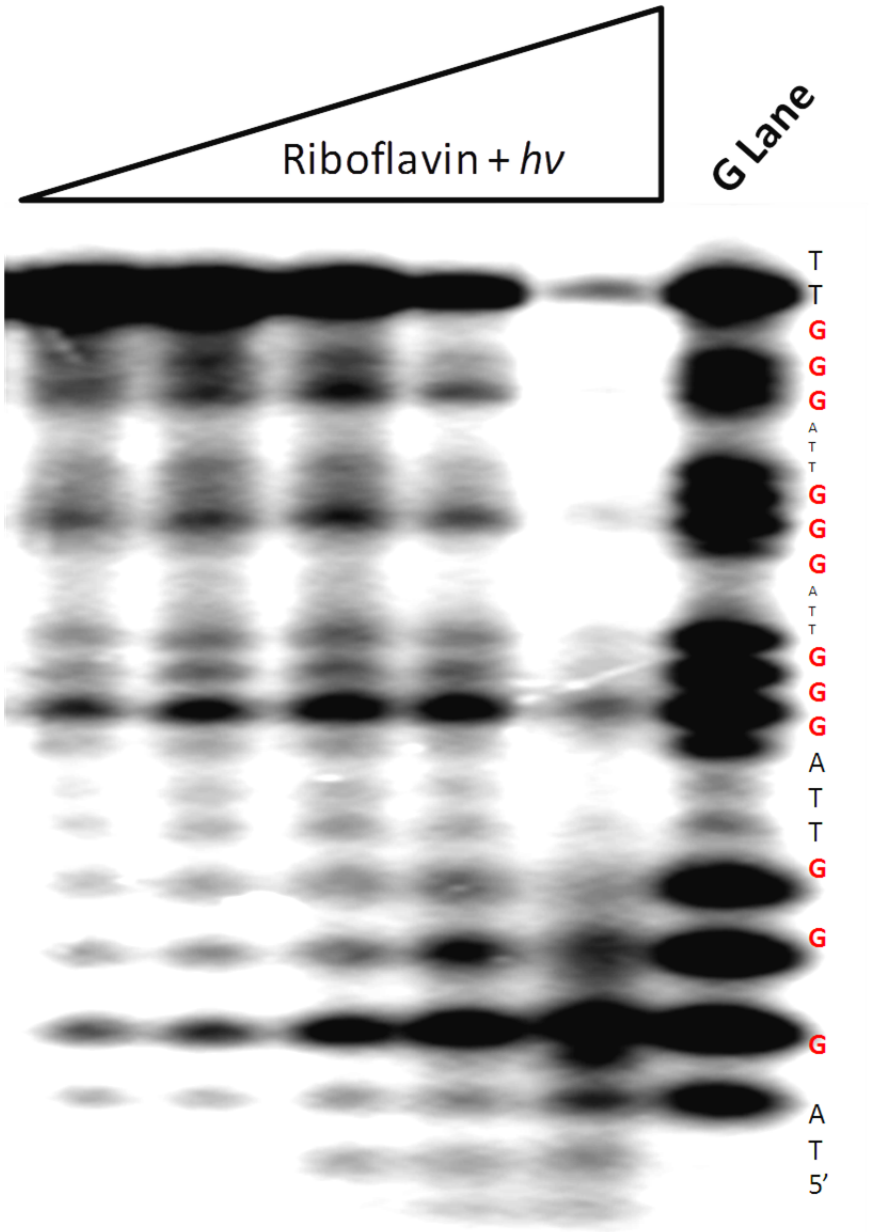

Figure S4. Representative storage-phosphor autoradiogram for the G-quadruplex oxidation sites. The data shown is the hybrid G-quadruplex oxidation with riboflavin and light (350 nm) with increasing irradiation time from left to right.

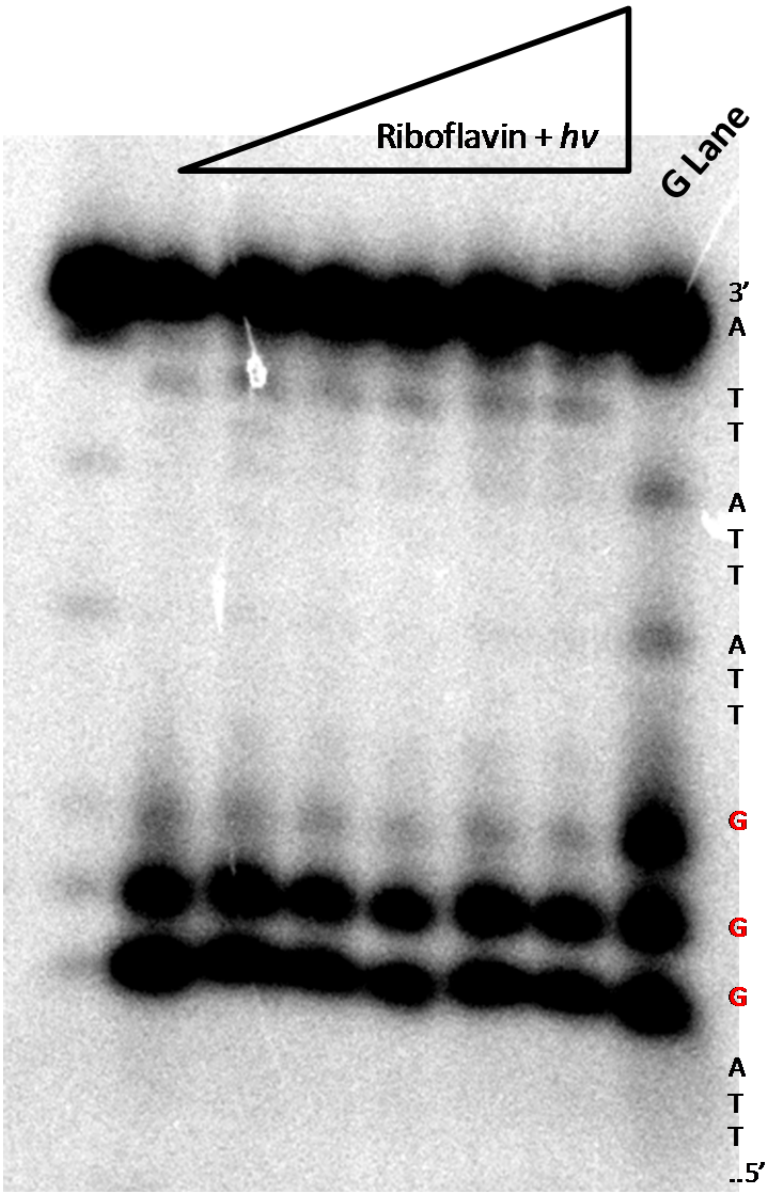

5'-ATA TTA TTA GGG TTA TTA TTA-3'
3'-TAT AAT AAT CCC AAT AAT AAT-5'

Figure S5. Representative storage-phosphor autoradiogram for the duplex oxidation sites with riboflavin. The data shown is the duplex oxidation with riboflavin and light (350 nm) with increasing irradiation time from left to right.

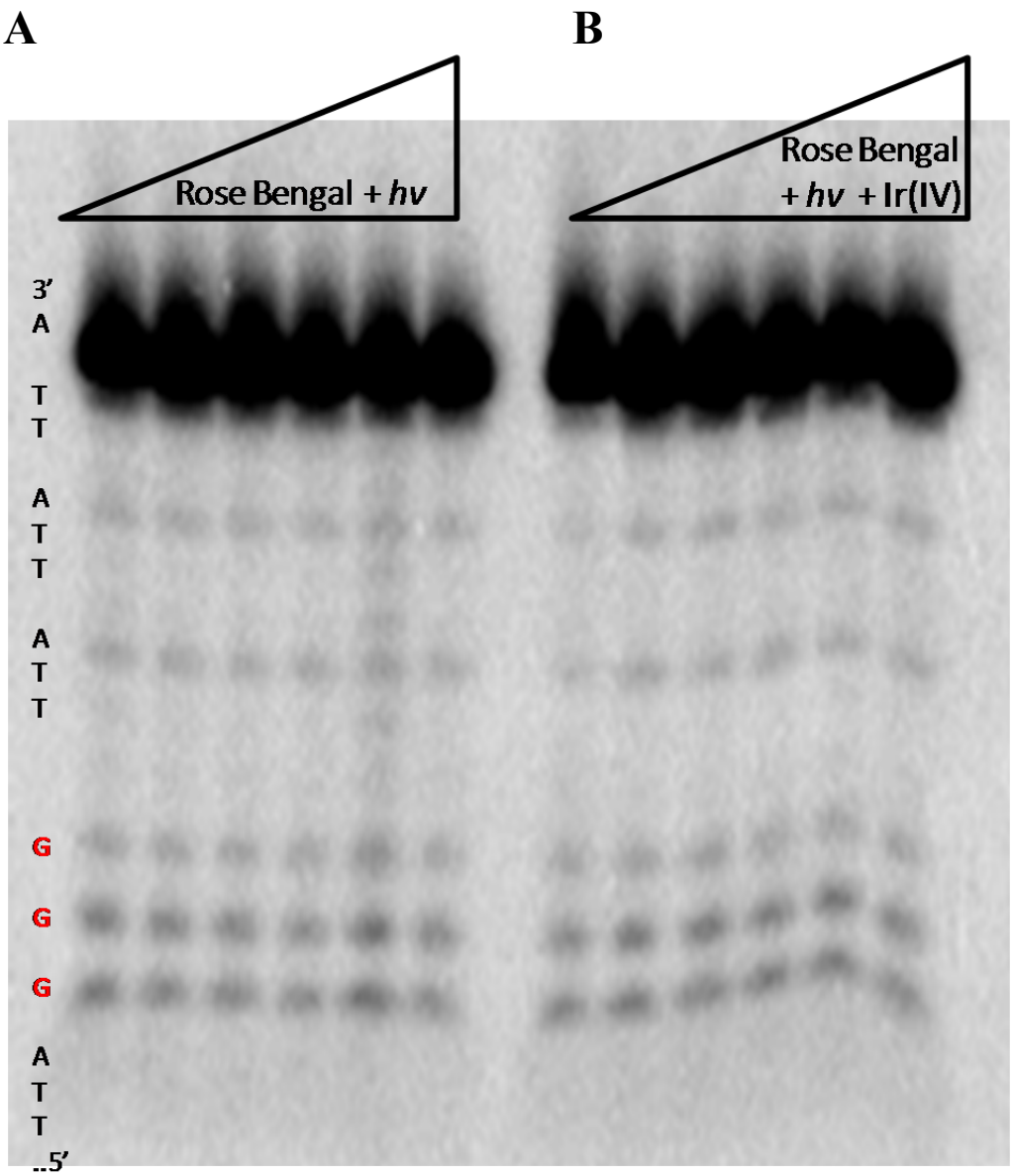

5'-ATA TTA TTA GGG TTA TTA TTA-3'
3'-TAT AAT AAT CCC AAT AAT AAT-5'

Figure S6. Representative storage-phosphor autoradiogram for the duplex oxidation sites with Rose Bengal. The data shown is the duplex oxidation with (A) Rose Bengal and light (350 nm), and (B) Rose Bengal and light (350 nm) and Na_2IrBr_6 (Ir(IV)). Increasing irradiation time is shown from left to right.

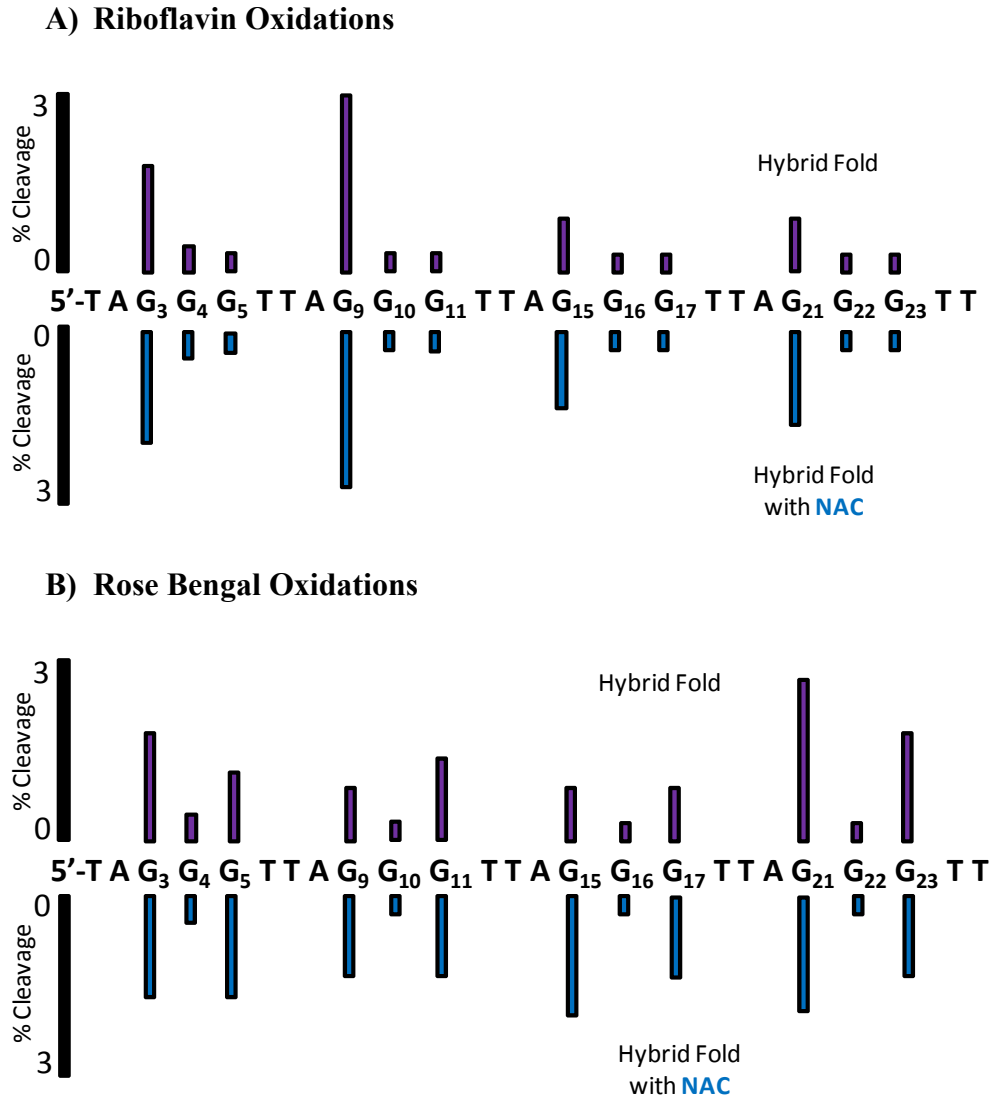

Figure S7. Comparison of oxidation sites for reactions conducted with and without NAC. (A) Riboflavin-mediated oxidations, and (B) is Rose Bengal-mediated oxidations. The data was conducted at ~12% conversion, with an error of ~20%.

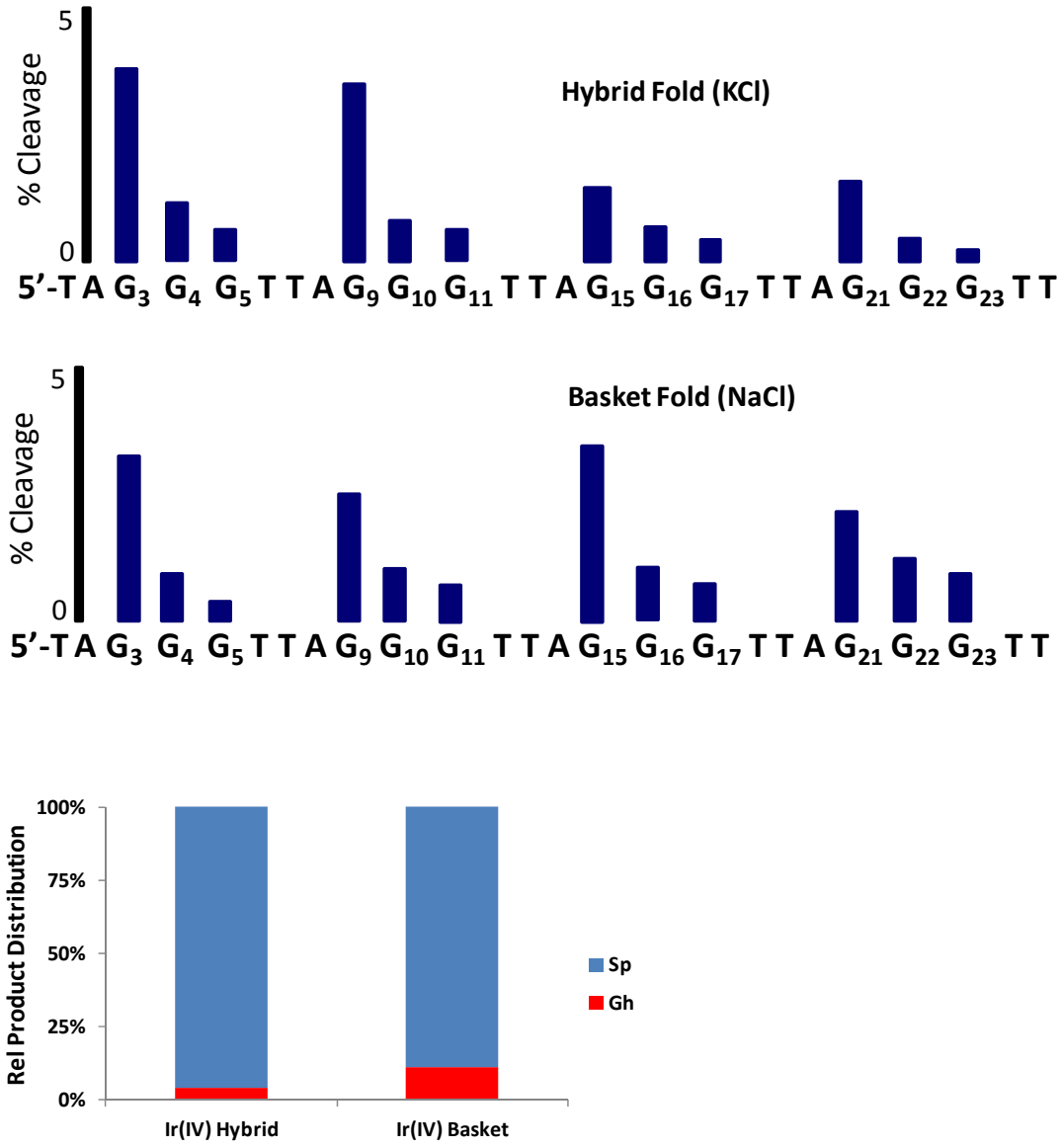

Figure S8. Oxidation sites and products observed in the hybrid and basket folds utilizing the one-electron oxidant Na_2IrCl_6. These studies were conducted at ~12% conversion to product with ~20% error.

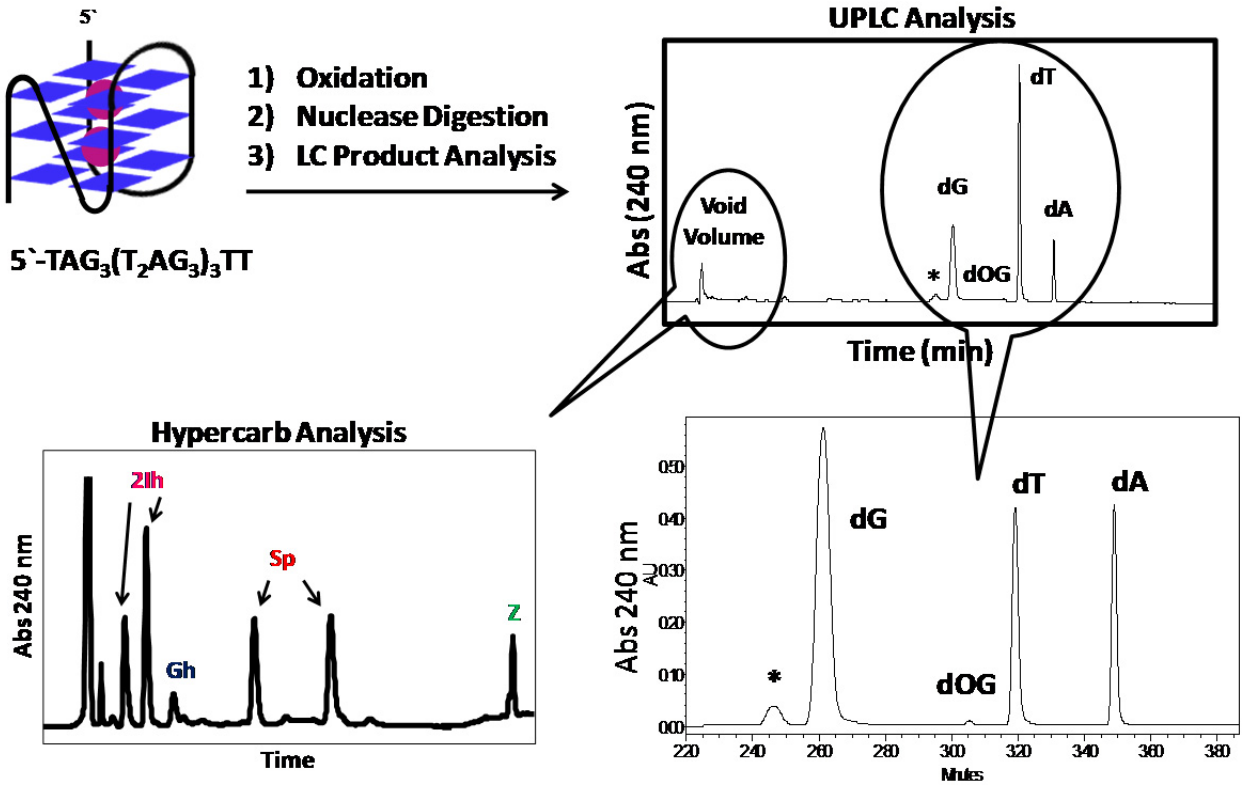

Figure S9. Method for determining the product distributions. *This peak is 2'-deoxyinosine, which results from deaminase impurities found in commercial nucleases.[2] We followed a method previously reported by our laboratory.[3]

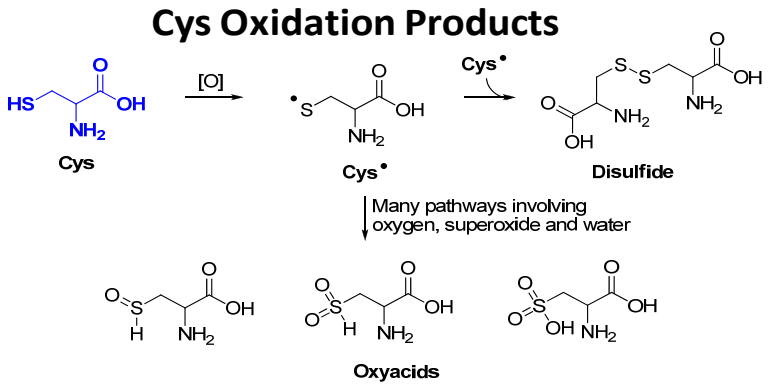

Davies, M.J. *Photochem. Photobiol. Sci.* **2004**, *3*, 17-25.

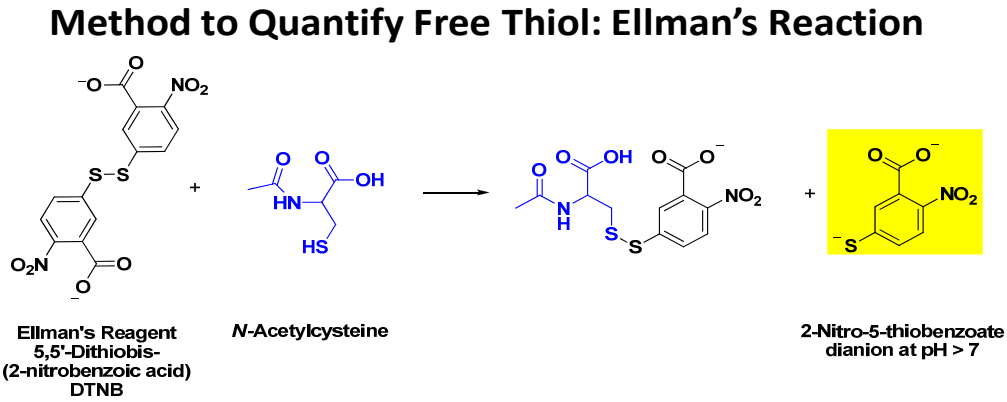

Bulaj, G.; Kortemme, T.; Goldenberg, D. P. *Biochemistry* **1998**, *37*, 8965-8972.

Standard curve for determination of free thiol concentrations

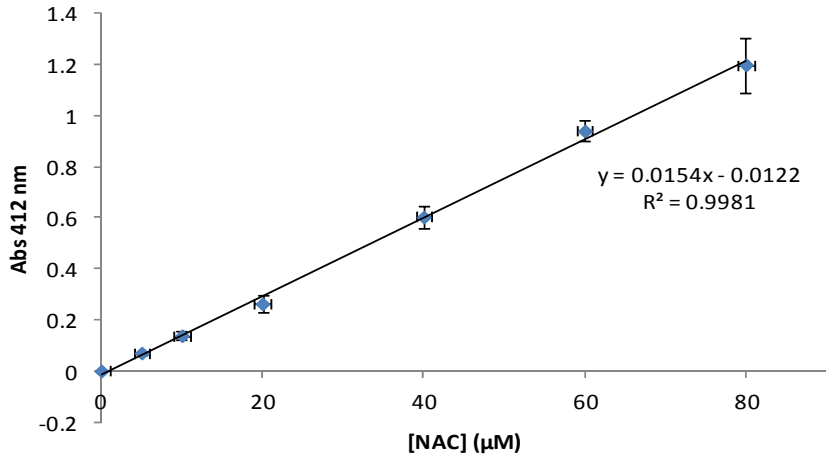

Reaction conditions: 0-80 µM NAC, 100 µM DTNB, and 200 mM Tris (pH 8.4) were mixed in a total volume of 1 mL. After letting the reaction proceed at 22 ^{o}C for 10 min the absorbance at 412 nm was measured.

Figure S10. Standard curve for Ellman's free thiol concentration test.

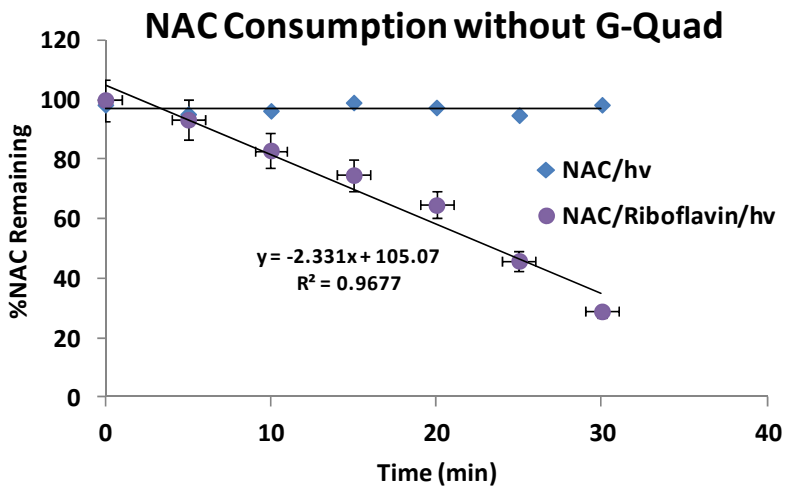

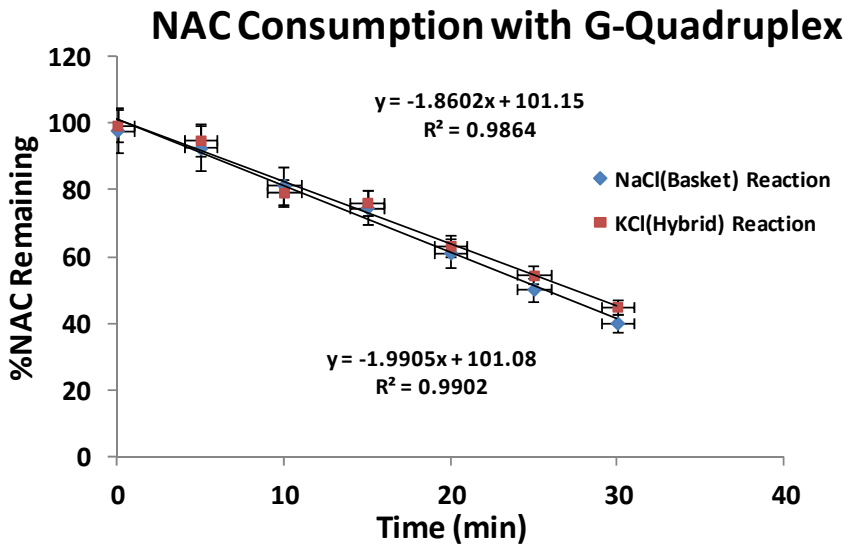

Oxidant	Reaction time for product determination	%NAC Remaining
Riboflavin + *hv*	20 min	57 ± 6%
Rose Bengal + *hv*	15 min	63 ± 7%

Reaction Conditions: A 25-µL aliquot of the reaction was mixed with 100 µM DTNB, and 200 mM Tris (pH 8.4) in a total volume of 1 mL. After letting the reaction proceed at 22 ^{o}C for 10 min the absorbance at 412 nm was measured.

Figure S11. Time-dependent concentrations of NAC during the oxidation reactions.

HPLC chromatogram for G*-T* crosslink standard

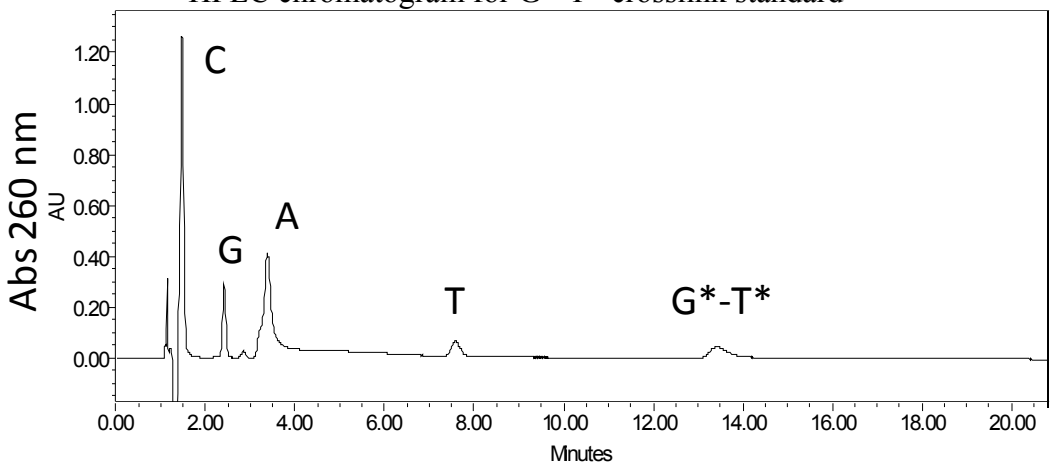

The G*-T* crosslink was synthesized in the ssODN 5'-CCTACGCTACC following a previously described method.[4] Briefly, 20 50-µL reactions containing a 10 µM solution of the ODN was mixed with 300 mM $NaHCO_3$ (pH 7.5) and 10 mM $K_2S_2O_8$. The samples were irradiated with 254 nm light for 3 h at 22 ^oC in Eppindorf tubes with the lids open. Next, the reactions were combined and dialyzed overnight to remove the excess salt. After lyophilization to dryness the sample was subjected to HF/pyridine hydrolysis (70% HF) in a 50-µL reaction at 37 ^oC for 30 min. The reaction was then neutralized by adding 1 mL ddH_2O and 80 mg of $CaCO_3$ while vortexing vigorously for 5 min. Finally, the sample was centrifuged and the supernatant was decanted and dried down. HPLC analysis was achieved using mobile phase A = 30 mM ammonium formate pH 3.5 and B = CH_3CN. The method was initiated at 0%B that was held isocratic for 10 min followed by a linear gradient to 20%B over the next 10 min.

HPLC chromatogram for a hydrolyzed G-qaudruplex oxidation reaction by carbonate radical that was generated with the SIN-1/HCO_3^- system.

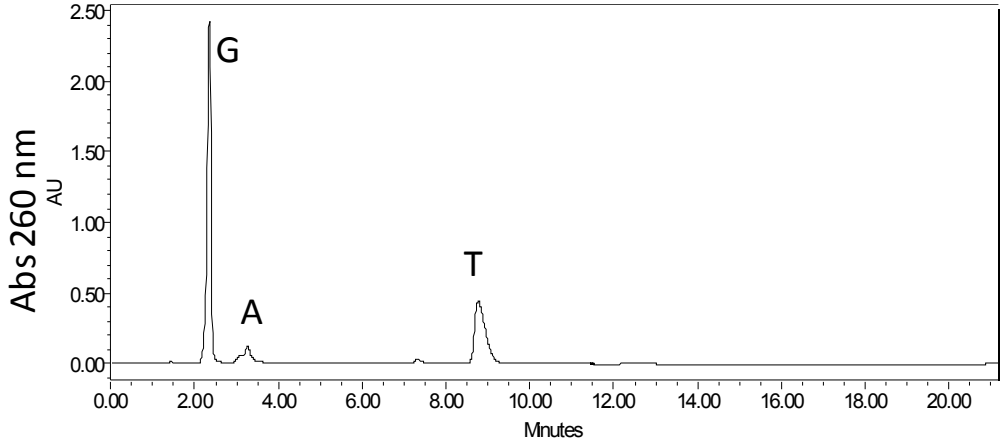

Figure S12. Hunt for a G*-T* crosslink.

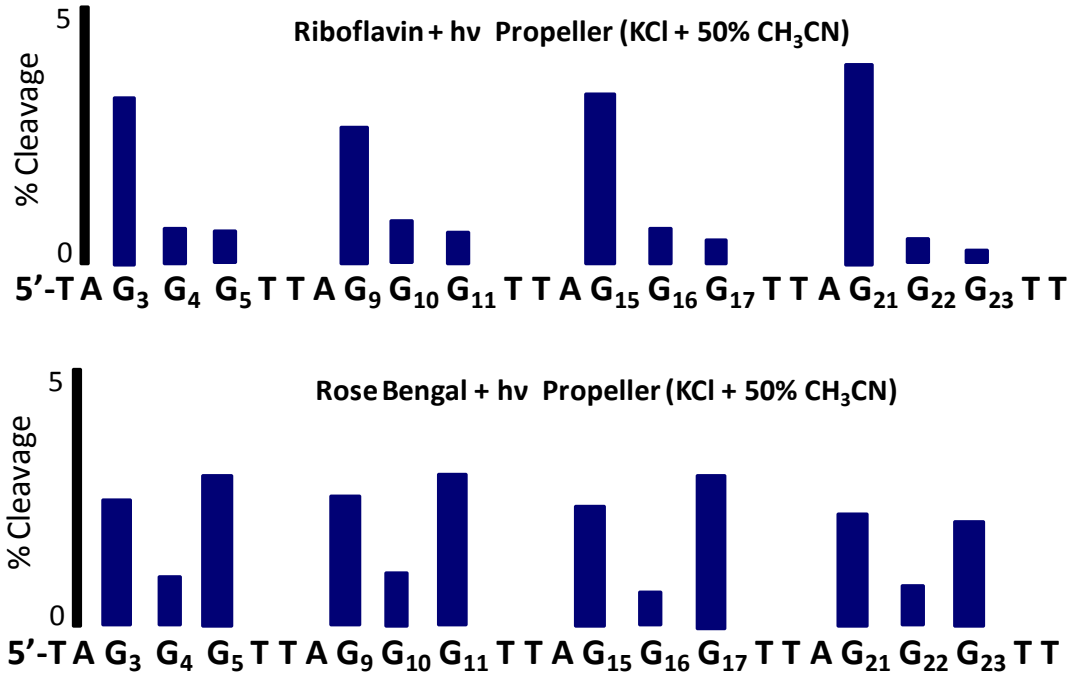

Figure S13. Oxidation sites observed for the propeller-like folded G-quadruplex.

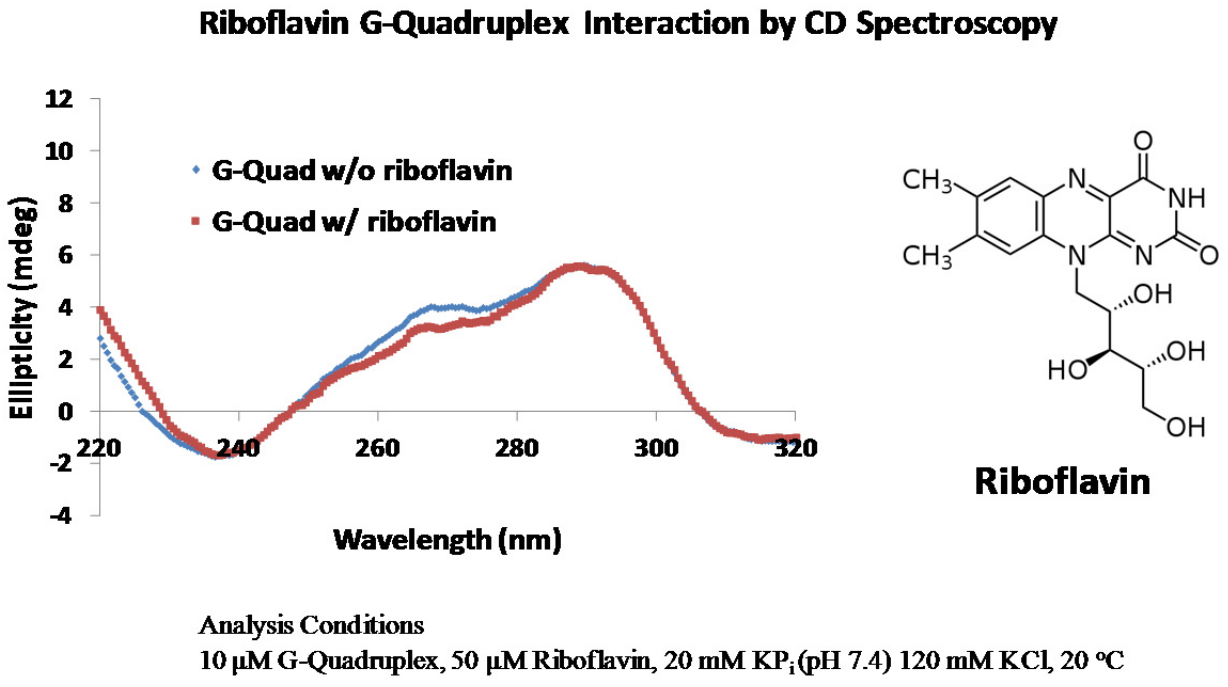

Figure S14. CD Spectra for G-quadruplexes in the presence of riboflavin. This experiment was conducted to address concerns about riboflavin interacting with the G-quadruplex under identical reaction conditions.

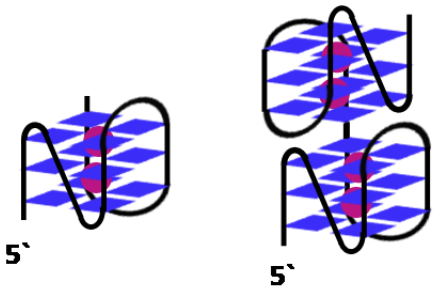

Sequence	T_m, N = 3	T_m, N = 7	Analysis Conditions	Ref
5`-TA GGG (TTA GGG)$_N$ TT	60.5 ± 0.7 °C	54.1 ± 0.9 °C	1 µM DNA in 20 mM KP_i (pH 7.4) 120 mM KCl.	–
5`-GGG (TTA GGG)$_N$	67 °C	63 °C	1 µM DNA in 10 mM KP_i (pH 7.0) 150 mM KCl.	6
5`-TTA GGG (TTA GGG)$_N$	62 °C	57 °C	1 µM DNA in 50 mM Tris (pH 7.0) 100 mM KCl.	5

Figure S15. CD and T_m characterization of the double G-quadruplex. Our data is similar to that published in the literature,[5, 6] and the CD spectra are similar to that reported in the literature.[7]

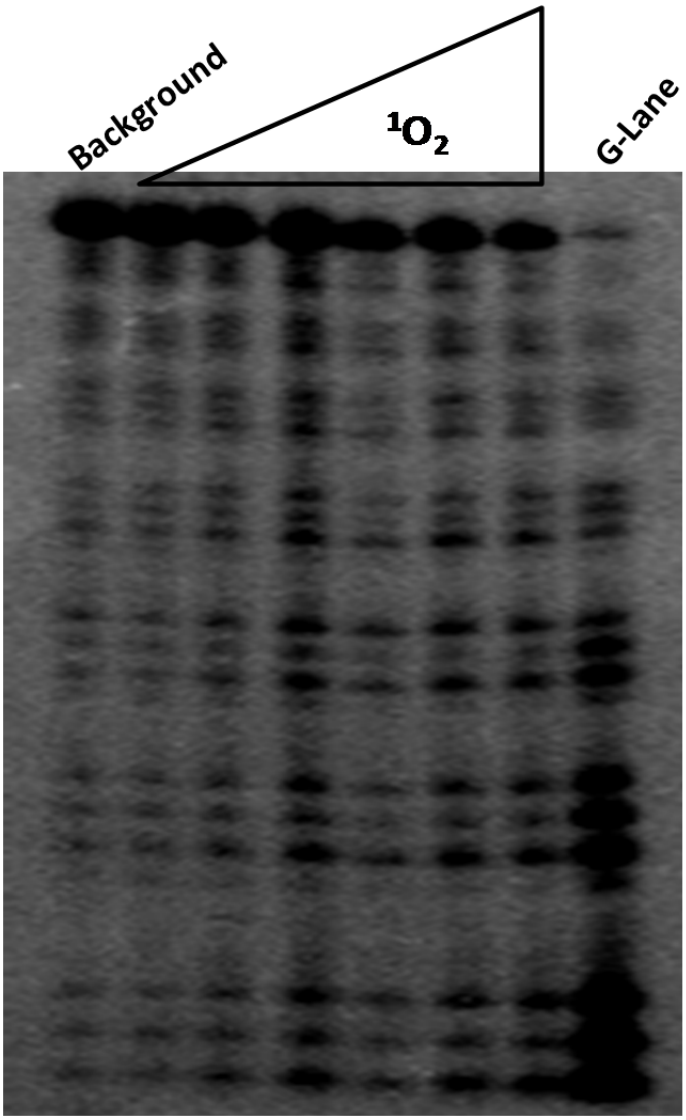

Figure S16. Gel-electrophoresis analysis of double-G-quadruplex oxidations with Rose Bengel ($^1O_2$). The sequence studied was 5'-TAGGG(TTAGGG)$_7$TT. Oxidations were conducted with 10 μM ODN 5 μM Rose Bengal, 20 mM KP_i (pH 7.4), 120 mM KCl at 37 ^oC.

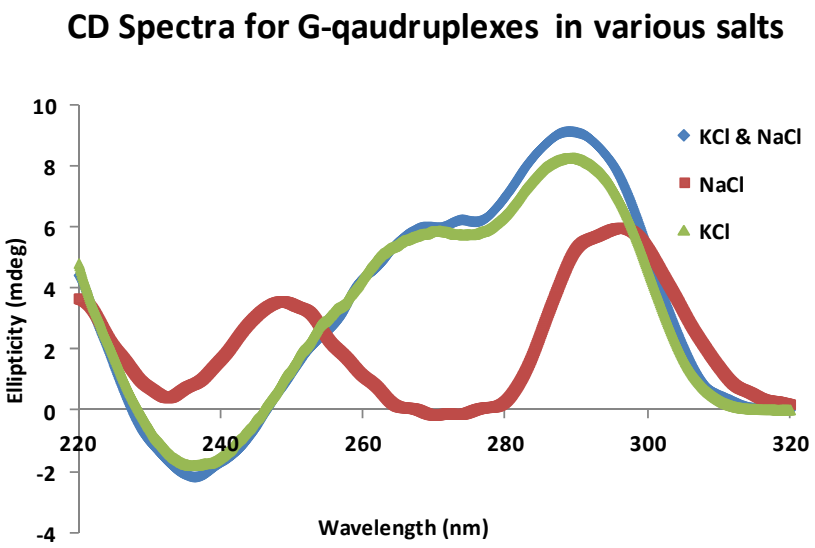

[Salt]	T_m (°C)
KCl (150 mM)	63.7 ± 0.3 °C
NaCl (150 mM)	56.0 ± 0.7 °C
KCl (140 mM) NaCl (12 mM)	64.5 ± 0.4 °C

Analysis Conditions-
20 mM MP_i (pH 7.4)
130 mM MCl, 10 µM DNA
(CD was conducted at 20 °C) (M = Na or K)

Or 20 mM KP_i (pH 7.4),
120 mM KCl + 12 mM NaCl

5`-TAGGG(TTAGGG)$_3$TT

Figure S17. Characterization of G-quadruplexes in mixed salts.

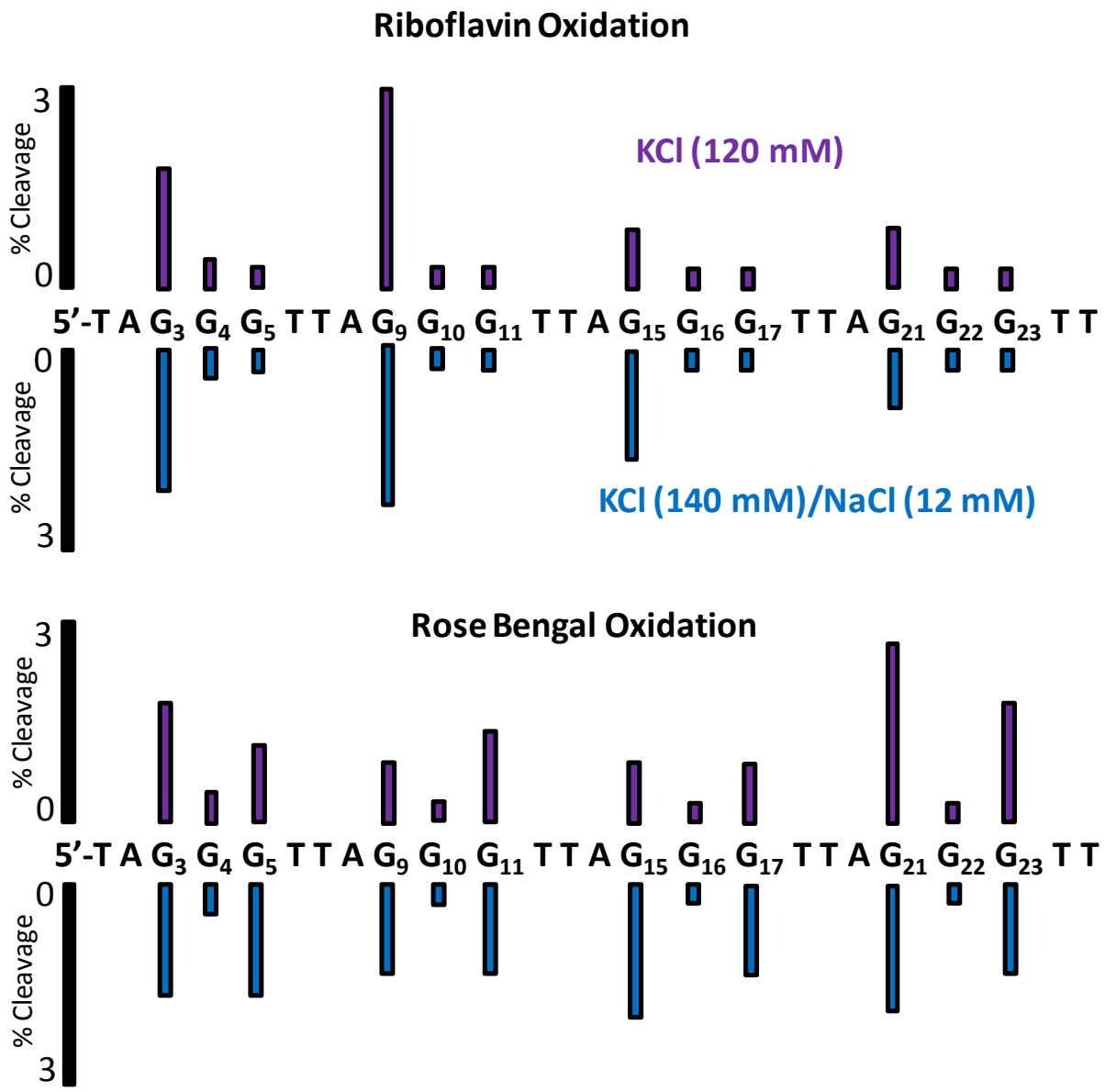

Figure S18. G-Quadruplex oxidation sites in mixed salt buffers.

Reevaluation of Sp and Gh extinction coefficients at 240 nm.
We elected to reconfirm our extinction coefficients used for Sp and Gh by co-injecting equimolar amounts of the hydantoins onto the hypercarb column (Thermo Fisher 150 X 4.6, 5 µm). This allowed us to directly compare the peak areas for Sp and Gh under the analysis conditions (0.1% acetic acid), which provided a direct comparison of Sp and Gh's relative extinction coefficients. Further, this is important because of the pH dependence in the extinction coefficients, which has previously been documented by our laboratory.[1, 3, 8, 9] This experiment was achieved by oxidizing OG with Na_2IrCl_6, as previously described, that effected 100% conversion to product without over oxidizing the Gh,[1] which was accomplished by monitoring the loss of OG by HPLC. Next, equal amounts of the Sp and Gh reactions were mixed and inject on the hypercarb column while monitoring their peak areas (see figure).

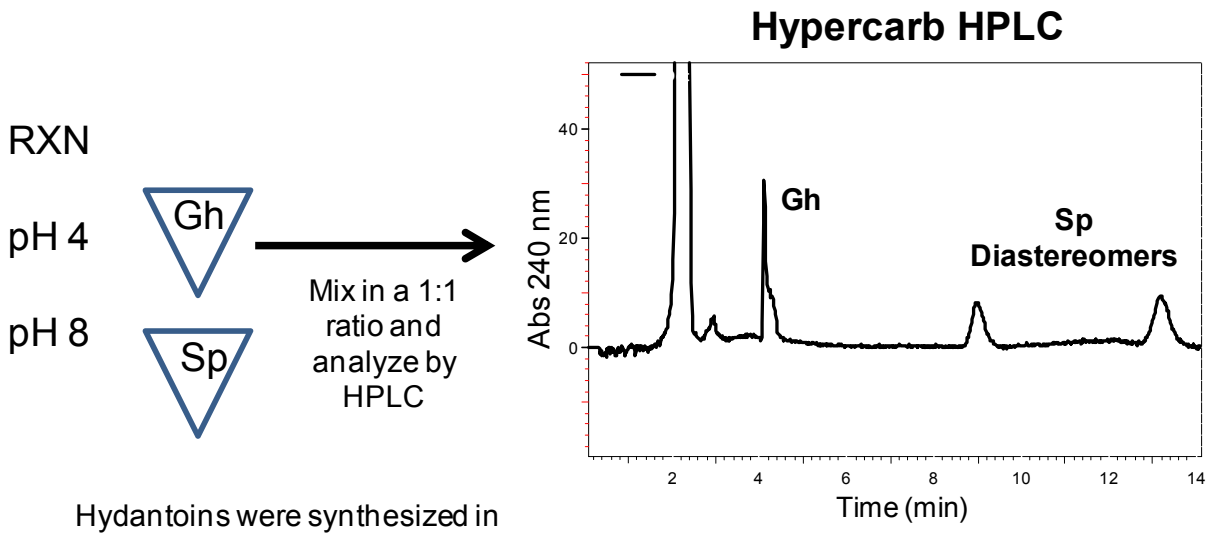

Hydantoins were synthesized in 100 mM of the appropriate buffer with 3 equiv of Na_2IrCl_6. 100% conversion of dOG was monitored by RP-HPLC

HPLC conditions: isocratic 100% A, where A = 0.1% acetic acid in ddH_2O pH 4

	Sp / Gh
Ratio of $\varepsilon_{240\ nm}$ values [a]	1.35
Ratio of HPLC areas	1.42 ± 0.12

[a] See references 8,9 for the reported Sp and Gh extinction coefficients adjusted to pH 4

Figure S19. Reevaluation of the Sp and Gh extinction coefficients.

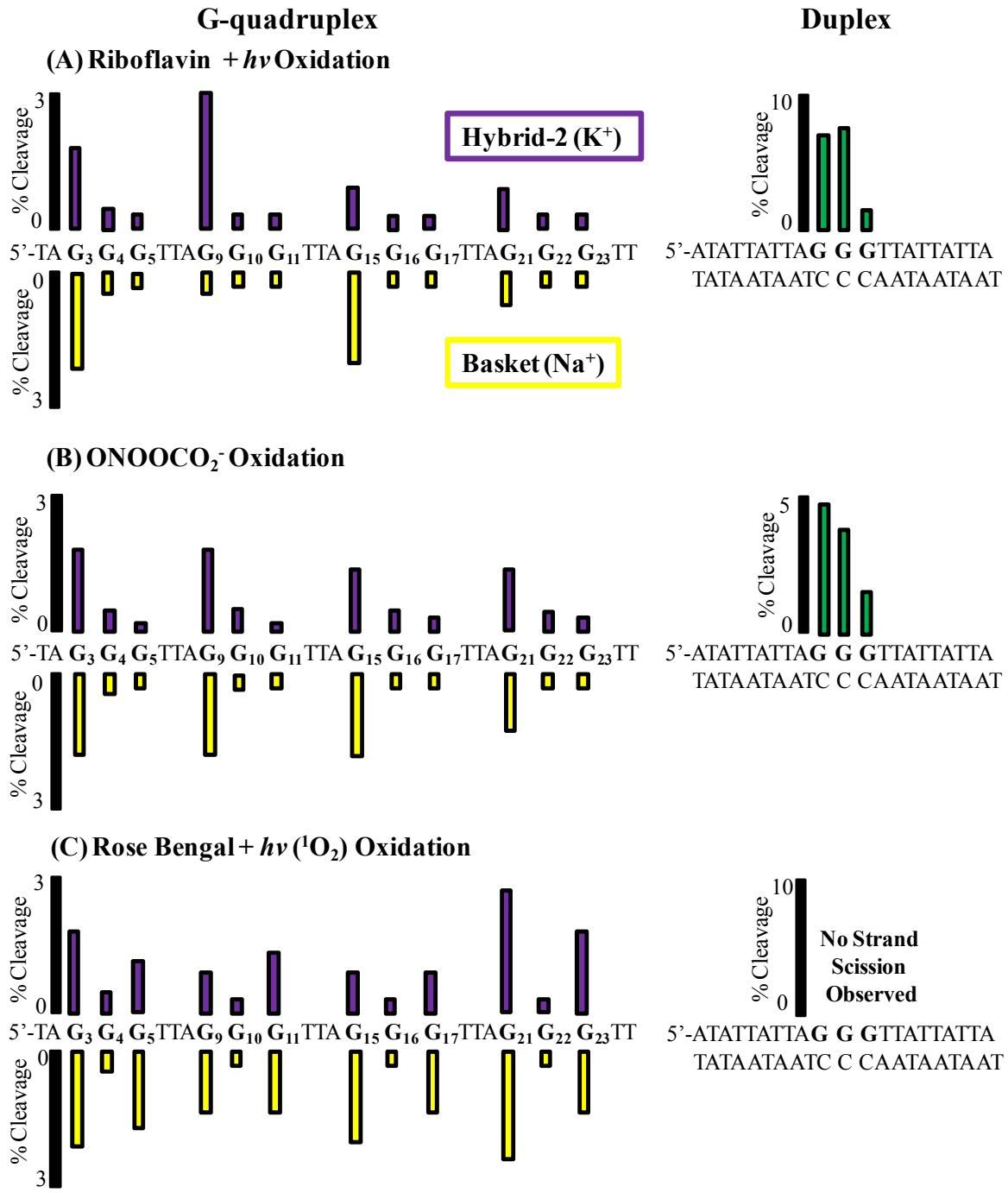

Figure S20. Comparison of reaction sites for the hybrid and basket folds.

Riboflavin-mediated Oxidations

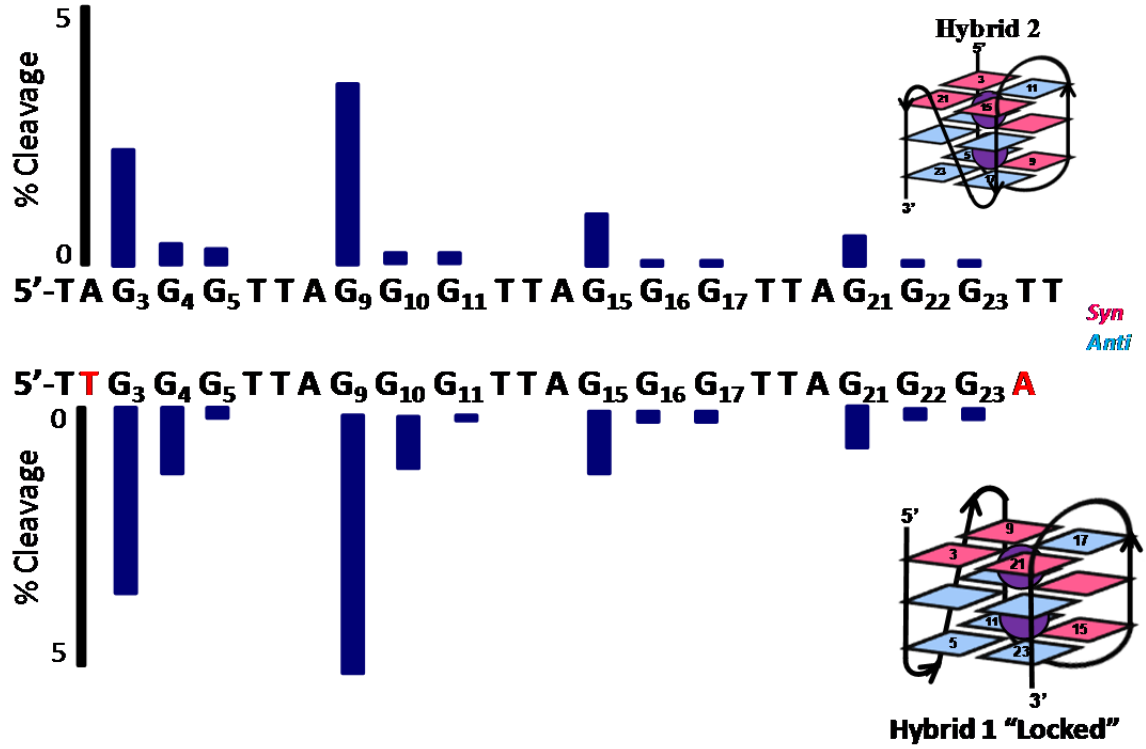

Based on NMR studies conducted by the Petal laboratory placement of a TT dinucleotide tail on the 5'-end and an A nucleotide on the 3'-end locks the telomere sequence in the hybrid-1 conformation.[10] The data presented above was conducted utilizing riboflavin + *hν* as the photooxidant.

Figure S21. Comparison of reaction sites for the natural human telomere sequence and the locked telomere sequence.

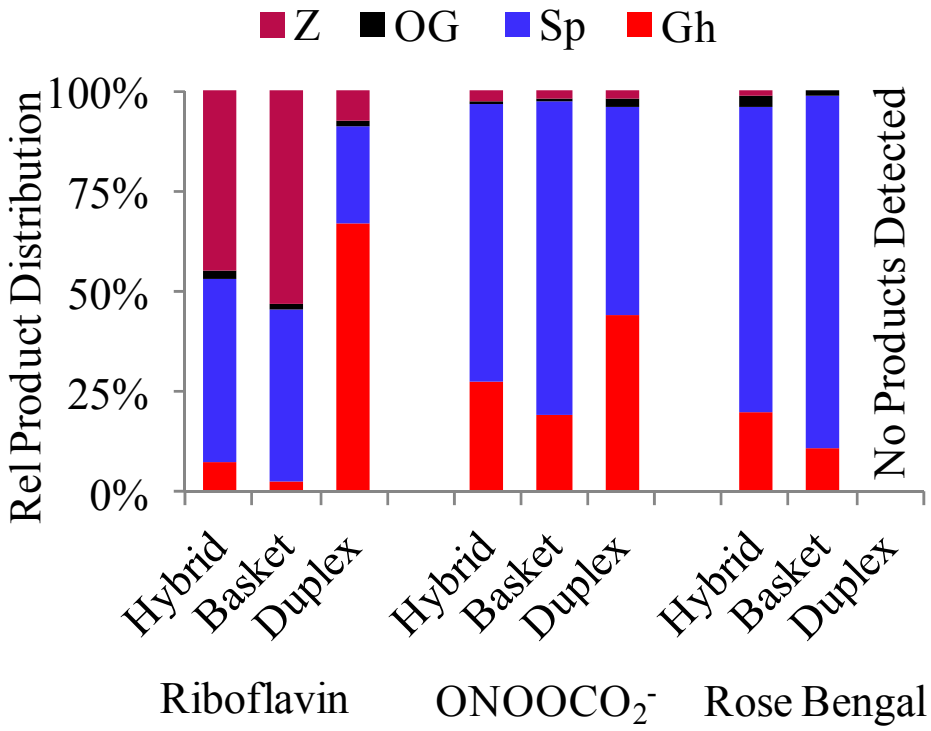

Figure S22. Relative product distributions for the contexts studied.

References

(1) Fleming, A. M.; Muller, J. G.; Dlouhy, A. C.; Burrows, C. J. (2012) Context effects in the oxidation of 8-oxo-7,8-dihydro-2'-deoxyguanosine to hydantoin products: Electrostatics, base stacking, and base pairing. *J. Am. Chem. Soc. 134*, 15091-15102.
(2) Taghizadeh, K.; McFaline, J. L.; Pang, B.; Sullivan, M.; Dong, M.; Plummer, E.; Dedon, P. C. (2008) Quantification of DNA damage products resulting from deamination, oxidation and reaction with products of lipid peroxidation by liquid chromatography isotope dilution tandem mass spectrometry. *Nat. Protocols 3*, 1287-1298.
(3) Fleming, A. M.; Muller, J. G.; Ji, I.; Burrows, C. J. (2011) Characterization of 2'-deoxyguanosine oxidation products observed in the Fenton-like system Cu(II)/H2O2/reductant in nucleoside and oligodeoxynucleotide contexts. *Org. Biomol. Chem. 9*, 3338-3348.
(4) Crean, C.; Uvaydov, Y.; Geacintov, N. E.; Shafirovich, V. (2008) Oxidation of single-stranded oligonucleotides by carbonate radical anions: generating intrastrand cross-links between guanine and thymine bases separated by cytosines. *Nucleic Acids Res. 36*, 742-755.
(5) Yu, H.-Q.; Miyoshi, D.; Sugimoto, N. (2006) Characterization of structure and stability of long telomeric DNA G-quadruplexes. *J. Am. Chem. Soc. 128*, 15461-15468.
(6) Vorlickova, M.; Chladkova, J.; Kejnovska, I.; Fialova, M.; Kypr, J. (2005) Guanine tetraplex topology of human telomere DNA is governed by the number of (TTAGGG) repeats. *Nucleic Acids Res. 33*, 5851-5860.
(7) Petraccone, L.; Trent, J. O.; Chaires, J. B. (2008) The tail of the telomere. *J. Am. Chem. Soc. 130*, 16530-16532.
(8) Luo, W.; Muller, J. G.; Rachlin, E. M.; Burrows, C. J. (2001) Characterization of hydantoin products from one-electron oxidation of 8-Oxo-7,8-dihydroguanosine in a nucleoside model. *Chem. Res. Toxicol. 14*, 927-938.
(9) Luo, W.; Muller, J. G.; Rachlin, E. M.; Burrows, C. J. (2000) Characterization of spiroiminodihydantoin as a product of one-electron oxidation of 8-oxo-7,8-dihydroguanosine. *Org. Lett. 2*, 613-616.
(10) Luu, K. N.; Phan, A. T.; Kuryavyi, V.; Lacroix, L.; Patel, D. J. (2006) Structure of the human telomere in K^+ solution: An intramolecular (3 + 1) G-quadruplex scaffold. *J. Am. Chem. Soc. 128*, 9963-9970.